Trans Indian Inst Met (2024) 77(6):1455–1465
https://doi.org/10.1007/s12666-023-03247-y

REVIEW

Research Progress on Composition Design of Multicomponent Eutectic High Entropy Alloys

Shiguang Wan[1] · Pan Ma[1,2] · Hong Yang[1] · Nan Zhang[1] · Yacheng Fang[1] · Yandong Jia[3] · K. G. Prashanth[4,5]

Received: 11 September 2023 / Accepted: 20 December 2023 / Published online: 23 February 2024

Abstract Eutectic high-entropy alloys (EHEAs) have unique properties, making them a significant sub-branch of HEAs. Researchers are interested in their high strength, good castability, and ductility. However, due to the lack of a complete phase diagram database and previous research results, the traditional trial-and-error method will greatly reduce the research efficiency, and the composition design of EHEAs faces many difficulties. This paper summarizes the recent proposals of the thermo-dynamic factors that have a decisive role in the design of EHEAs. Regarding previous research, we discussed the methods for designing the main eutectic compositions currently used in research. These methods aid in developing novel approaches to fabricating EHEAs.

Keywords Eutectic high-entropy alloys · Component design · Thermodynamic parameters · Phase diagram simulation

✉ Pan Ma
mapan@sues.edu.cn

1 School of Materials Science and Engineering, Shanghai University of Engineering Science, Shanghai, China

2 State Key Laboratory of Advanced Welding and Joining, Harbin Institute of Technology, Harbin 150001, China

3 Laboratory for Microstructures, Institute of Materials, Shanghai University, Shanghai 200444, China

4 Department of Mechanical and Industrial Engineering, Tallinn University of Technology, Ehitajate tee 5, 19086 Tallinn, Estonia

5 CBCMT, School of Mechanical Engineering, Vellore Institute of Technology, Vellore, Tamil Nadu 630014, India

1 Introduction

In 2004, Yeh and Cantor et al. proposed a new class of alloy system, namely high-entropy alloys (HEAs) [1]. Unlike traditional alloy systems, high-entropy alloys are usually composed of at least four principal elements, so they have extremely high mixing entropy. According to the second law of thermodynamics, the mixing configuration entropy per mole can be expressed as, $\Delta S_{mix} = -R\sum_{i=1}^{n} c_i \ln c_i$ [2], where R is the gas constant, c_i is the mole fraction of the i-th element, and n is the total number of constituent elements. According to the "high entropy" effect, when multiple principal elements are mixed in equimolar fractions, random solid solutions with stable compounds are formed [3, 4]. It is noted from previous research that mixing multiple elements in HEAs results in high entropy, lattice distortion, sluggish diffusion, and cocktail effects. Specifically, the presence of a high entropy plays an important role in simplifying the micro-structures so that they principally consist of a simple solid solution with structures like body-centered cubic (*bcc*)/face-centered cubic (*fcc*). The distortion of the lattice has a significant impact on the mechanical, physical, and chemical properties of alloys. This can cause sluggish diffusion, resulting in the development of nanocrystalline or amorphous structures. Additionally, the combination of different elements can create a composite effect on properties, with interactions between the elements playing a crucial role [2]. However, the strength and ductility of traditional high-entropy alloys are difficult to balance at the same time. In previous studies, high-strength alloys show compromised ductility and vice-versa [5–7]. In order to balance the shortcomings of this traditional high-entropy alloy, the concept of eutectic high-entropy alloys (EHEAs) was proposed by Lu et al. in 2014, which has become the most important sub-branch in the field of high-entropy alloy research [8–10].

The *fcc* phase provides enough plasticity for the alloy, and the *bcc* phase makes the alloy have excellent strength, and EHEAs that consist of both soft *fcc* and hard *bcc* or intermetallic phase provide ideal strength and ductility (usually showing a layered or rod-like structure). Eutectic alloys offer several advantages including: (1) a microstructure that is resistant to changes at high temperatures, (2) low-energy phase boundaries, (3) the ability to control the microstructure, (4) high fracture strength, (5) a stable defect structure, (6) good resistance to creep at high temperatures, and (7) a regularly layered or rod-like eutectic structure that forms an in-situ composite material [11].

In recent years, due to the presence of an excellent two-phase equilibrium system of EHEAs, it has attracted recent attention. However, the traditional trial-and-error and experimental methods seem to be unable to meet the current needs. During the design and development of EHEAs, the influence of many thermodynamic parameters on the formation of the eutectic phase must first be considered [12]. Therefore, it is very important to determine reasonable parameters to generate a stable eutectic phase, such as mixing entropy (ΔS_{mix}), mixing enthalpy (ΔH_{mix}) and atomic size difference (δ_r), and valence electron concentration (VEC) are the factors that form multiple key influencing factors for the phase formation [13–15].

Recently, researchers have designed some methods to explore the components of EHEAs, including the simple mixing method [16, 17], mixing enthalpy method [12], CALPHAD-assisted method [20–25], and solidification process simulation [26–31]. These methods are mainly based on the phase diagram and solidification process simulation mainly with the help of Thermo-calc, JmatPro, and Pandat software. Furthermore, experimental experiences are often used in compositional design, especially for the design and fabrication of Co-free EHEA [32–35]. Apart from the above said conventional design methods, a new infinite solid-solution strategy was proposed by Ye et al., [36] and four EHEAs with excellent compressive mechanical properties were successfully designed, namely NiAl–20V–17Cr, NiAl–30V–5Mo, NiAl–30Cr–Mo and NiAl–20V–10Cr–5Mo. An EHEA with seven components was designed by Shah et al. using an integrated computational materials engineering (ICME)-based framework [37]. A method combining machine learning (ML) and thermodynamic calculations to quickly locate the eutectic composition in the Ni–Co–Cr–Al system was proposed by Liu et al. [38]. A Co-free and cost-effective EHEA based on the valance electron concentration (VEC) criterion was designed by Wu et al. [39]. Three EHEAs of $Al_{20.45}Co_{10}Cr_{10}Ni_{59.55}$, $Al_{17.5}Co_{20}Cr_{20}Ni_{52.5}$, and $Al_{16.3}Co_{25}Cr_{25}Ni_{33.7}$ were designed by Liu et al. based on the pseudo-ternary phase diagram and microscopic observation [40]. This paper mainly reviews the main components of the EHEA phases fabricated in recent years and the physical factors affecting phase formation and discusses and analyzes the proposed alloy design methods.

2 Thermodynamic Parameter(s) for Multicomponent Alloy Formation

During the solidification process of the eutectic phase, in order to ensure the stability of the eutectic phase formation, some empirical physical parameters are proposed to design the alloy composition, such as mixing entropy ΔS mix, mixing enthalpy ΔH mix, atomic size difference δr and valence electron concentration VEC [13, 14]. Table 1 lists the alloys with fully eutectic composition and the above empirical physical parameters discovered in recent years. We have also carried out computational verification on them. Below we will discuss their calculation methods and the references provided for the design of eutectic phase formation.

2.1 Mixing Entropy

According to Boltzmann's hypothesis, the formula for calculating the configurational entropy change per mole (ΔSmix) during solid solution formation from n elements with equimolar fractions is [1, 13]:

$$\Delta S_{mix} = -R \sum_{i=1}^{n} \left(C_i \ln C_i \right) \tag{1}$$

The formula for calculating the mole percent of a component, C_i, involves adding up the values of C subscript i from i equals 1 to n. In this equation, the equipment control is equal to 4, and the gas constant, R, is 8.314 $J{\cdot}K^{-1}$ mol^{-1}. When dealing with equiatomic ratio alloys, the entropy of mixing reaches its maximum. This means that multi-component HEAs with equal or nearly equal atomic ratios have a significantly higher entropy of mixing compared to conventional alloys. According to Zhang et al., when $12 \leq \Delta S_{mix} \leq 17.5$ J/mol, it is easy to form a solid solution [14]. Thus at high values of ΔS_{mix} at sufficiently high temperatures, a particular solid solution phase is stable [12].

2.2 Mixing Enthalpy

The equation for determining the enthalpy of mixing in a multi-component alloy system with n elements is:

$$\Delta H_{mix} = \sum_{i=1, i \neq j}^{n} \Omega_{ij} c_i c_j \tag{2}$$

where Ωij $(=4\Delta H_{AB}^{mix})$ is the regular solution interaction parameter between the *i*-th and *j*-th elements, c_i or c_j is the atomic percentage of the *i*-th or *j*-th component, ΔH_{AB}^{mix} is

Table 1 Eutectic phase composition of eutectic high-entropy alloy (EHEA) and calculated values of its thermodynamic parameters ΔSmix, ΔHmix, δr and VEC

Alloy composition	Eutectic Phases	ΔS_{mix} (J/mol·K)	ΔH_{mix} (kJ/mol)	δ_r (%)	VEC	Refs.
$Al_{1.3}CrFeNi$	BCC + B2	11.47	− 14.26	6.59	6.49	[46]
$CrFeNi_{2.2}Al_{0.8}$	FCC + B2	10.79	− 12.21	5.36	7.68	[32]
$Fe_{20}Co_{20}Ni_{41}Al_{19}$	FCC + BCC	11.02	− 12.23	5.70	8.07	[47]
$Al_{19.4}Co_{20.6}Cr_{20.6}Ni_{39.4}$	FCC + B2	11.11	− 14.31	5.67	7.61	[22]
$Fe_{35}Ni_{25}Cr_{25}Mo_{15}$	FCC + Laves	11.18	− 4.27	3.35	7.70	[34]
$AlCr_{1.3}TiNi_2$	BCC + $L2_1$	11.16	− 26.25	7.36	7.32	[48]
$Al_{0.9}CoFeNi_2$	FCC + B2	11.02	− 11.93	5.63	8.10	[49]
$Al_{17}Ni_{34}Ti_{17}V_{32}$	BCC + $L2_1$	11.09	− 28.40	6.32	6.19	[50]
$AlCoCrFeNi_{2.1}$	FCC + B2	12.91	− 11.94	5.38	7.70	[8]
$Al_{0.7}CoCrFeNi$	FCC + B2	13.31	− 10.57	5.18	7.47	[51]
$AlCrFeNiMo_{0.2}$	BCC + B2	12.57	− 12.65	6.50	6.71	[52]
$AlCrFeNiCo_{1.9}$	FCC + B2	13.04	− 11.33	5.42	7.47	[24]
$CoCrFeNiNb_{0.65}$	FCC + Laves	13.28	− 11.22	5.56	7.80	[53]
$CoCrFeNiNb_{0.45}$	FCC + Laves	13.08	− 10.59	4.90	7.92	[54]
$Nb_{0.73}CoCrFeNi_{2.1}$	FCC + Laves	12.76	− 12.46	4.76	8.30	[55]
$CoCrFeNiZr_{0.5}$	FCC + Laves	13.14	− 15.45	8.38	7.78	[56]
$CoCrFeNiTa_{0.395}$	FCC + Laves	13.00	− 11.91	4.16	7.96	[57]
$CoCrFeNiTa_{0.43}$	FCC + Laves	13.06	− 12.25	4.30	7.93	[58]
$CoCrFeNiMo_{0.8}$	FCC + Laves	13.35	− 10.92	3.43	7.87	[59]
$Co_2Mo_{0.8}Ni_2VW_{0.8}$	FCC + Laves	12.65	− 8.30	4.90	7.97	[60]
$Co_{20}Cu_{20}Fe_{20}Ni_{20}Ti_{20}$	FCC + Laves	13.38	− 9.44	6.50	8.40	[61]
$Co_{25}Fe_{25}Mn_5Ni_{25}Ti_{20}$	FCC + Laves	12.57	− 17.72	6.71	7.90	[62]
$Al_{28}Cr_{20}Nb_{15}Ti_{27}Zr_{10}$	B2 + Laves	12.86	− 22.01	6.94	4.27	[29]
$CoFeNi_2V_{0.5}Nb_{0.75}$	FCC + Laves	12.48	− 15.91	5.80	8.27	[63]
CoCrFeNiMnPd	FCC + Laves	14.90	− 7.67	3.36	8.33	[19]
$Ni_{30}Co_{30}Cr_{10}Fe_{10}Al_{18}W_2$	FCC + B2	13.05	− 12.20	5.59	7.76	[64]
$Co_{25.1}Cr_{18.8}Fe_{23.3}Ni_{22.6}Ta_{8.5}Al_{1.7}$	FCC + Laves	13.43	− 9.76	4.40	7.99	[65]
$(Co_{40}Cr_{10}Fe_5Mo_5Ni_{40})_{82.2}Al_{17.8}$	FCC + B2	12.52	− 12.68	5.59	7.85	[25]
$Ni_{1.5}CrCoFe_{0.5}Mo_{0.1}Nb_{0.68}$	FCC + Laves	13.45	− 13.46	5.07	7.95	[28]
26.75Fe–25Ni–15Cr–10Co–10V–5Mn–8.25Ta	FCC + Laves	14.97	− 10.90	4.38	7.70	[37]

the binary alloy mixing enthalpy [13]. In the calculation, the mixing enthalpy value ΔH_{AB}^{mix} is based on the Miedema macroscopic model of the binary liquid alloy, which can be obtained elsewhere [41]. Intermetallic phases form when the enthalpy of mixing between constituent elements is highly negative. Conversely, phases separate when enthalpy of mixing is positive or less negative [42]. Therefore, a reasonable mixing enthalpy value can ensure the formation of a stable eutectic phase. For the formation of solid solution and intermetallic phases in EHEAs, negative mixing enthalpy and high mixing entropy are required. [43].

2.3 Atomic Size Difference

When there are significant variations in the sizes of atoms present, it can result in significant distortion of the lattice and can decrease the stability of solid solutions. This can also intensify the lattice hysteresis effect of high-entropy alloys and increase the likelihood of a segregation effect occurring. To describe the size difference of atoms inside an n element alloy, the introduction of the atomic size difference factor (δ) is expressed as follows:

$$\delta = \sqrt{\sum_{i=1}^{n} c_i \left(1 - \frac{r_i}{\bar{r}}\right)^2} \tag{3}$$

where c_i is the atomic percentage of the i^{th} component, $\bar{r} = \sum_{i=1}^{n} c_i r_i$ is the average atomic radius, and c_i values may be obtained from elsewhere [13, 44]. The parameter δ is also crucial for predicting the phase formation, a smaller value of δ is preferable for the creation of solid solutions with a single phase. Since EHEAs have a dual-phase structure, the value of δ should not be small, and a eutectic dual-phase structure is formed when $\delta > 3\%$ [12].

2.4 Valence Electron Concentration

The phase stability of alloy systems depends on electron concentration, which can be determined by VEC or valence electrons (*e/a*), the average number of itinerant electrons per atom. The valence electron concentration (VEC) of multi-component alloys can be calculated as the *e/a* ratio of the constituent components or the weighted average of VEC. Since HEAs mainly contain transition metals, and the *e/a* of transition metals is controversial, follow-up studies are all based on VEC [45]. In order to study the effect of VEC on the phase equilibrium of HEA, the VEC of multi-element HEA can be determined by the following formula:

$$VEC = \sum_{i=1}^{n} c_i VEC_i \tag{4}$$

where VEC_i is the VEC of a single element, this can be obtained by looking up the periodic table of elements. According to the research of Chanda et al., the VEC of EHEAs should be kept in the range of $6 \le \mathrm{VEC} \le 8.5$, which facilitates the formation of a two-phased eutectic structure (*fcc* + *bcc* phase) [12].

3 Summary

To accurately obtain the dual-phase structure of EHEAs, the physical thermodynamic method is used as the guiding tool. Therefore, determining a reasonable mixing entropy, mixing enthalpy, atomic size difference, and VEC is crucial for the formation of the eutectic phase. According to previous reports, higher ΔS_{mix} and negative ΔH_{mix} are necessary for the formation of the solid solution and intermetallic phases in EHEAs. However, the value of δ should be relatively large, and higher δ can aggravate lattice distortion and lead to the destabilization of simple phases in EHEAs. Specifically, the eutectic structures in various HEAs are formed under the following conditions: $-18 \le \Delta H_{mix} \le -6$, $6 \le \mathrm{VEC} \le 8.5$, and $\delta_r > 3$ [12, 43]. According to Eqs. (1–4), we calculated these physical parameters for EHEAs with all-eutectic composition from four to seven components proposed in recent years, as shown in Table 1. To view the influence of EHEAs thermodynamic parameters on phase transition more clearly and intuitively, Fig. 1 lists the relationship between two typical thermodynamic parameters, atomic size difference and mixing enthalpy. Clearly, the ingredients that form a typical two-phase eutectic high-entropy alloy are located in the red marked area. For *fcc* + Laves/*bcc* phased EHEAs, the mixing enthalpy is in line with the general situation, lower than − 7 kJ/mol and greater than − 18 kJ/mol. When the mixing enthalpy is too large, lower than − 18 kJ/mol, it is difficult to form a *fcc* solid solution, and it can also be understood that it is easy to form an ordered intermetallic compound with low mixing entropy and high mixing enthalpy, as shown in the green area in Fig. 1 [66].

4 Design Methods for Eutectic High Entropy Alloys

Since EHEAs exhibit an excellent balance of plasticity and ductility, the development of EHEAs has attracted attention in recent years. So far thermodynamic parameters-based methods (discussed above) have been extensively utilized, in addition to phase diagram calculations, etc. The applicable scenarios using the existing composition design methods

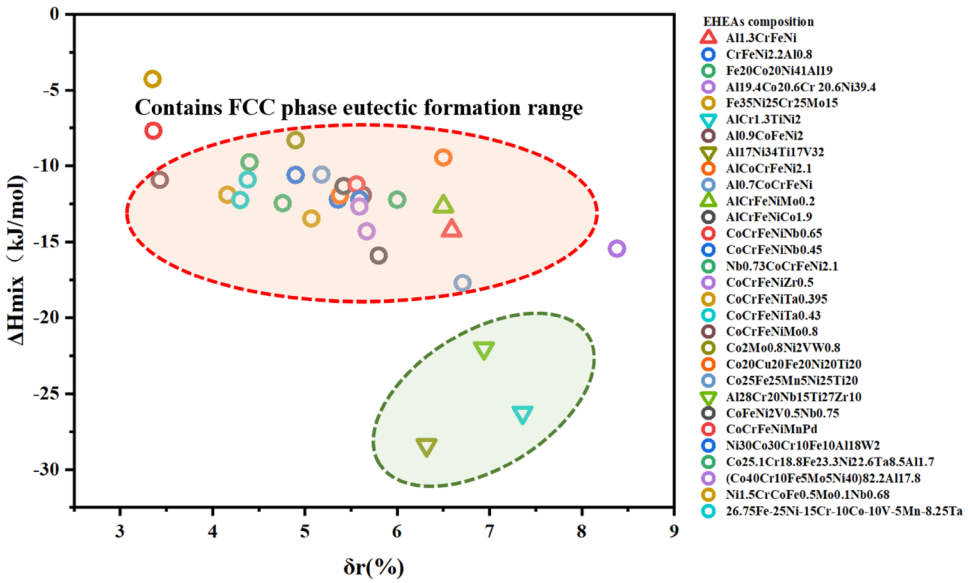

Fig. 1 Plot displaying the correlation between the difference in atomic size (δr) and the mixing enthalpy (ΔHmix) of eutectic high-entropy alloys (EHEAs)

and their limitations will be discussed in detail in this short review.

4.1 Simple Mixing Method

Jiang et al. [16] proposed the simple mixing method, a new design strategy that uses mixing enthalpy and binary eutectic composition to locate eutectic composition in HEA. According to previous studies, it is known that CoCrFeNi alloys have a simple *fcc* solid solution structure in the cast state, and is called CoCrFeNi high-entropy base elements (HEBE), and elements with larger enthalpy mixed with CoCrFeNi (such as ZrNbTaHfAl) are called eutectic forming elements (EFE) [67]. By consulting the binary mixing enthalpy table, it is shown that the mixing enthalpy (ΔH_{mix}) between Nb, Ta, Zr, and Hf elements and Co, Cr, Fe, and Ni elements is very negative. In addition, by finding the elements contributing to the formation of the eutectic phase are identified. Finally, by combining binary eutectic compositions in a 1:1 equimolar ratio, four new EHEAs, namely $CoCrFeNiNb_{0.6}$, $CoCrFeNiTa_{0.47}$, $CoCrFeNiZr_{0.51}$, and $CoCrFeNiHf_{0.49}$, were designed. The structure on display is a combination of *fcc* and Laves phases, forming a eutectic composition. Thereafter, based on this idea, Xie et al. [68, 69] proposed an improved simple hybrid method to design some five-element $Co_aCr_bFe_cNi_d$-M (M is the EFE elements) EHEAs. Unlike before, the EFE elements are in non-equiatomic ratios. It first determines the eutectic point of each binary system, determines the parameters based on the simple mixing method, and finally obtains the full eutectic structure by fine-tuning the *x* value, the design idea is shown in Fig. 2. These studies showed good utility in the compositional design of EHEAs, but they were limited to the development of five-component EHEAs. To overcome this limitation, Jiao et al. [17] proposed a simple hybrid method for designing EHEAs with more than five elements. They created four new EHEAs, consisting of *fcc* and Laves phases: $CoCrFeNiNb_{0.25}Ta_{0.20}$, $CoCrFeNi–Ta_{0.25}Hf_{0.25}$, $CoCrFeNiNb_{0.15}Zr_{0.15}–Hf_{0.15}$ and $CoCrFeNiZr_{0.17}Hf_{0.16}Ta_{0.16}$.

4.2 Mixed Enthalpy Method

Lu et al. [18] proposed a new strategy to design EHEAs using mixing enthalpy, also known as the mixing enthalpy method. Due to the very negative mixing enthalpy of both Al and Ni in $AlCoCrFeNi_{2.1}$EHEA, Al is substituted with elements such as Zr, Nb, Hf, and Ta that have similar negative mixing enthalpy as Ni. Finally, the molar ratio of the elements is obtained through the inverse relationship between the element content and the mixing enthalpy, and finally, the new EHEAs composition is designed through fine-tuning. Four novel EHEAs with fully eutectic compositions of $Zr_{0.6}CoCrFeNi_{2.0}$, $Nb_{0.74}CoCrFeNi_{2.0}$, $Hf_{0.55}CoCrFeNi_{2.0}$, and $Ta_{0.65}CoCrFeNi_{2.0}$ were designed. They displayed a lamellar eutectic morphology consisting of *fcc* and laves dual phases, as depicted in Fig. 3. This method is highly effective and offers accurate results, and it was relatively easy to locate new EHEA components. However, it is only applicable to modify a few elements in the existing EHEA to obtain a new eutectic composition, and the scope of application is relatively narrow.

4.3 CALPHD Assisted Method

To design the eutectic alloy composition more accurately, He and his colleagues [20] proposed a method for designing the eutectic composition using the pseudo-binary phase diagram. First, it is necessary to find out the elements that form eutectic structures with single-phase HEA matrix elements, mainly through the existing binary or ternary phase diagram. Thermo-Calc software database is then utilized to calculate the pseudo-binary phase diagram, determine the phase formation process during solidification, obtain the eutectic composition, and finally verify the accuracy

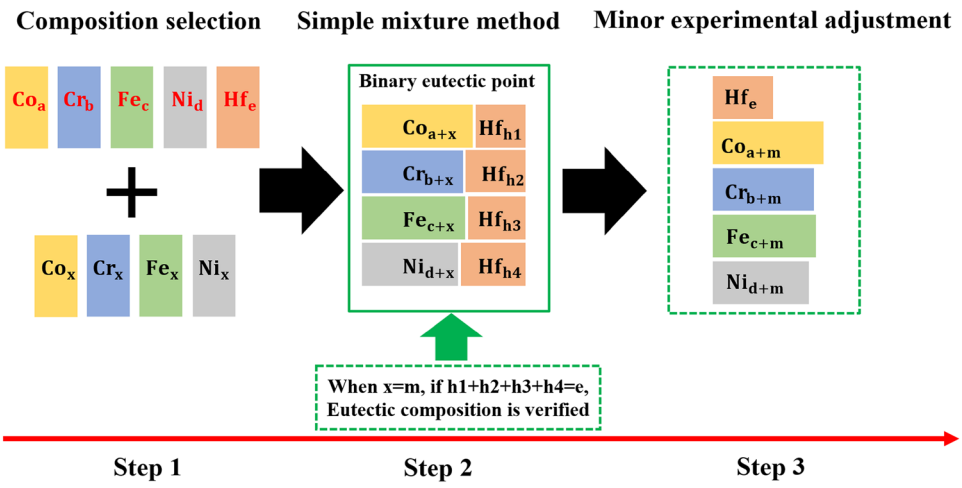

Fig. 2 Here is a diagram detailing the modified simple mixing method [68]

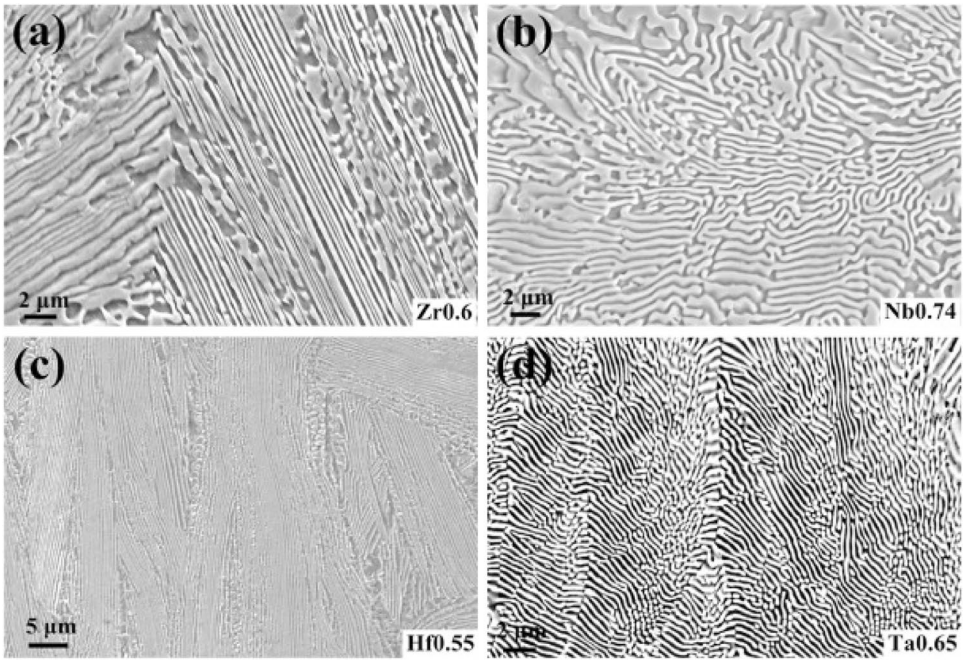

Fig. 3 Scanning electron microscopy images of four new EHEAs: **a** $Zr_{0.6}CoCrFeNi_{2.0}$, **b** $Nb_{0.74}CoCrFeNi_{2.0}$, **c** $Hf_{0.55}CoCrFeNi_{2.0}$, and **d** $Ta_{0.65}CoCrFeNi_{2.0}$, respectively [18]

of the theoretical results through experiments. According to this idea, the hypoeutectic structure of $CoCrFeNiNb_{0.5}$ was successfully designed. The results obtained matched well with the pseudo-binary phase diagram. In addition, Gasan and Ozcan used thermodynamic and computational methods to design new EHEAs [25]. To find the eutectic point, they considered 324 equilibrium phase diagrams and verified their thermodynamic factors. Finally, $(Co_{40}Cr_{10}Fe_5Mo_5Ni_{40})_{82.2}Al_{17.8}$ EHEAs with *fcc* and *B2* phase compositions were designed. Subsequently, Wu et al. [22] proposed a method for designing EHEA using CALPHAD. The method involved calculating pseudo-binary diagrams based on the eutectic group phase and establishing a pseudo-ternary phase diagram to guide alloy design. Pandat 2016.1 software and the PanHEA2017 database were used to create the CoCrNi–NiAl pseudo-binary and NiCo–Cr–NiAl pseudo-ternary phase diagrams. AlCoCrNi EHEAs with both *fcc* and *B2* phases were prepared using thermodynamic guidance. Layered and rod-like mixed eutectic microstructures were characterized. However, the results were inaccurate due to the imperfect database of CALPHAD. Hence, perfecting the database is crucial for the effective utilization of this design method.

The concept of alloy design with the assistance of CALPAHD is being developed. Mukarram et al. [23, 70] calculated the CoCrFeNi–Ta pseudo-binary phase diagram using Thermocalc software and the TCHEA database, and successfully developed eutectic and hypereutectic alloys with *fcc* and laves phase compositions. In addition, they evaluated the influence of Mo addition to CoCrFeNi and the resultant formation of a eutectic microstructure through pseudo-binary phase diagram calculations and successfully developed a eutectic consisting of *fcc* (A2) and intermetallic phases (σ and μ) through experiments ($CoCrFeNiMo_{0.5}$ and $CoCrFeNiMo_{1.0}$). Modifications in the CoCrFeNi–Ta pseudo binary phase diagram calculated with the help of Thermocalc software were made in view of the obtained experimental results, as shown in Fig. 4. Using the same database, Vikram et al. [24] designed and developed a Co-based EHEA using Thermo-Calc reproduced analytical calculations. Finally, using this method, CALPHAD is employed to verify or guide the EHEA composition design. Due to the relative imperfection of the database, as the number of constituent elements increases, the difficulty of establishing phase diagrams also increases. Therefore, this method cannot be directly used in the composition design of EHEAs like traditional binary and ternary alloys. In the process of pseudo-binary phase diagram simulation and needs fine-tuning. Therefore, for the design of EHEAs by the CALPHD-assisted method, the establishment of a comprehensive database and a considerable number of experimental conclusions are the key directions in the future.

4.4 Solidification Process Simulation

Wang et al. [31]. proposed a new method to design EHEA by calculating the solidification path (using JMatPro software), which mainly predicts the eutectic composition through solidification path analysis, and then verifies the accuracy of the results through experiments. Specifically, as shown in Fig. 5, The solidification paths of NiAl, bcc, and liquid are represented by black, orange, and blue

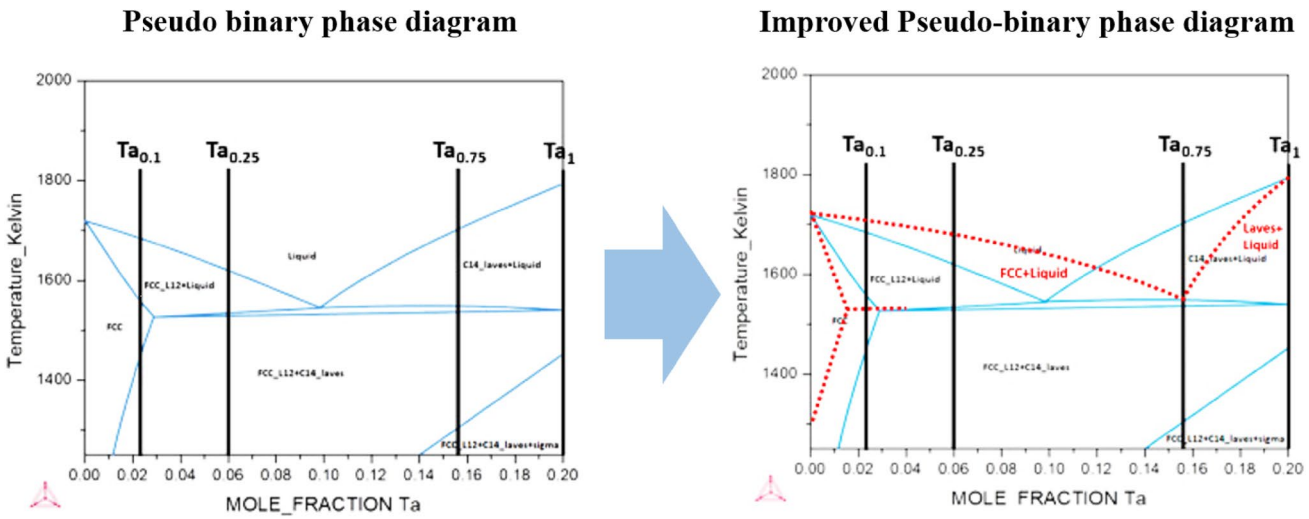

Fig. 4 Pseudo-binary Phase Diagram Adjustment of CoCrFeNi–Ta [23]

curves, respectively. There was no inflection point in the solidification cooling curves of the three components. Three EHEAs were successfully designed: NiAl–$Mo_{8.7}Cr_{8.7}V_{8.7}$, NiAl–$Mo_{14.5}Cr_{14.5}Fe_{14.5}$, and NiAl–$Mo_{10}Cr_{10}V_{10}Fe_{10}$. They consist of eutectic dendrites with B2 and bcc layered structures. No primary phase appears, but two phases (eutectic) solidify simultaneously.

Similarly, Ai et al. [26] designed $CoCrFeNiTa_x$ type EHEAs by analyzing binary phase diagrams and thermodynamic calculations (JMatPro). It is verified by experiments that the obtained $CoCrFeNiTa_{0.43}$ alloy has a layered eutectic phase composed of *fcc*/laves phase. In addition, Ali Shafiei proposed a simple method to predict the composition of the EHEA in the Al–Co–Cr–Fe–Ni system [30]. To verify the design process, the solidification process was simulated with JMatPro® software version 7.0.0. To determine the phase composition, Wen et al. [28] simulated the solidification process of the coating material (JmatPro). By adjusting the composition content, the $Ni_{1.5}CrCoFe_{0.5}Mo_{0.1}Nb_{0.68}$ EHEA with *fcc* phase and laves phase structure was designed.

Solidification process simulation accelerates composition design of EHEAs by quantitatively and visually determining eutectic and phase compositions of alloys. However, it cannot be used independently at present. Like the CALPHAD method, it is mostly used to verify the composition of known EHEAs alloy systems, and it still relies on past research results for newly developed alloys. Moreover, the obtained results also need to be fine-tuned due to the limitations of the thermodynamic database, as well as constraints such as the instability of the solidification process of the metal and the solid solubility of the metal elements.

4.5 Through Experimental Experience

In the composition design of EHEAs and to ensure their industrial applications, it is also necessary to consider saving materials cost and considering excellent performance. Approaches to designing new EHEAs using experience gained by adjusting elements of known alloys are also commonly used. Due to the high cost of Co, the engineering

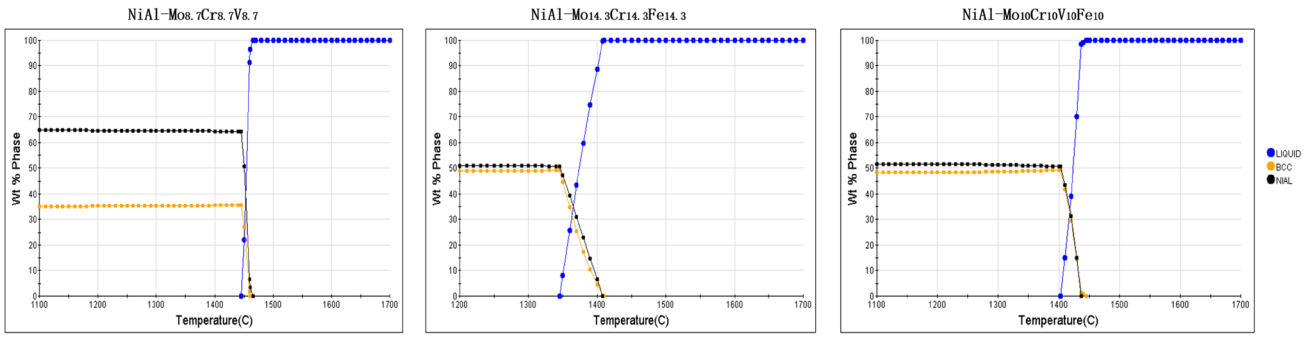

Fig. 5 Solidification paths for the NiAl–$Mo_{8.7}Cr_{8.7}V_{8.7}$, NiAl–$Mo_{14.3}Cr_{14.3}Fe_{14.3}$ and NiAl–$Mo_{10}Cr_{10}V_{10}Fe_{10}$ alloys calculated using JmatPro

application of some EHEAs is greatly limited. Therefore, Jin et al. [32] proposed a cost-effective method to create more than 10 potential Co-free EHEAs. The main idea is to replace Cobalt with Nickel. Nickel promotes the formation of the fcc phase, while Aluminum promotes the formation of the bcc phase [45]. The intermetallic phase-forming elements were modified. Multiple experiments were carried out to locate the eutectic point. As a result, a CrFeNi2.2Al0.8 eutectic HEA was successfully designed, composed of *fcc* and ordered *bcc* (B2) phases. Similarly, Dong et al. [33] designed $AlCrFeNi_3$ EHEAs with FeCrNi-type *fcc* and NiAl-type *B2* phases, maintaining good mechanical properties while reducing the materials' cost. In addition, Yin et al. [34] designed a new cost-effective $Fe_{35}Ni_{25}Cr_{25}Mo_{15}$ EHEA by avoiding the use of expensive Co and increasing the content of Fe. Jiao et al. [35] designed $Fe_2Ni_2CrMo_xEHEAs$ by equiatomic substitution while considering cost reduction and oxidation/corrosion resistance, showing a eutectic dual-phase structure when $x > 0.25$. Therefore, this method enables the design of specific alloy systems and is also instructive for the development of EHEA.

5 Summary

The above commonly used EHEAs design methods have their own scope of application and advantages and disadvantages in the process of actual component exploration, as shown in Table 2. In addition to the above design methods, researchers have begun to explore new design methods, mainly by optimizing and using the original design methods. Naishalkumar Shah et al. [37] developed an integrated computational materials engineering (ICME) framework for an EHEA consisting of seven components. The framework includes thermodynamic prediction using CALPHAD, phase field simulation for microstructure, and experimental validation. The predictions can be used for the design of HEA fabricated by various manufacturing processes. The alloy that was designed exhibits a eutectic structure comprising of *fcc* and laves phases. Based on ML methods and elemental classification results, Liu et al. [38] calculated and predicted the eutectic composition through CALPHAD, and obtained two new types of EHEA $Ni_{49}Co_{16}Cr_{16}Al_{19}$ and $Ni_{46.7}Co_{15}Cr_{20}Al_{18.3}$ through experimental verification. Ye et al. [36] proposed a new strategy for designing EHEAs with *B2* (NiAl phase) and *bcc* structures using infinite solid solution, which mainly generate phases by analyzing binary phase diagrams, four with seaweed eutectic dendritic microstructures. Several EHEAs were designed, including NiAl–20V–17Cr, NiAl–30V–5Mo, NiAl–30Cr–Mo and NiAl–20V–10Cr–5Mo using similar methods.

Recently, Wu et al. [39] maintained the VEC of the alloy by substituting Ni and Fe in equal proportions for Co in

Table 2 Applicable scope, advantages and disadvantages of common EHEAs design methods

Design method	Applicable scope	Advantage	Disadvantage
Simple mixing method	Five elements and more	A new idea of using binary eutectic to locate the eutectic point is proposed, and the composition positioning accuracy is high	Most of them are only suitable for the development of five elements, and the calculation of more than five elements is cumbersome
Mixed enthalpy method	Elemental fine-tuning of existing EHEAs	High efficiency of design and accuracy of results, and easier positioning of new EHEA components	The scope of application is narrow, only applicable to the adjustment of the existing eutectic composition
CALPHD Assisted Method	Element Adjustment of Alloy System in CALPHD Database	It has the advantage of developing new eutectic components, which can better verify or accelerate the design of EHEAs components	The database is not perfect, the more elements there are, the greater the relative error, resulting in inaccurate results
Solidification process simulation	Validation of known alloy systems	The determination of eutectic composition is more quantitative and visualized, which accelerates the design process of EHEAs	Inaccurate results due to instabilities in the metal solidification process
Through experimental experience	Alloy systems for specific applications	Designing EHEAs with Industrial Applications in mind	Only fine-tuning the composition of the existing alloy system can only be verified by traditional experimental trial and error

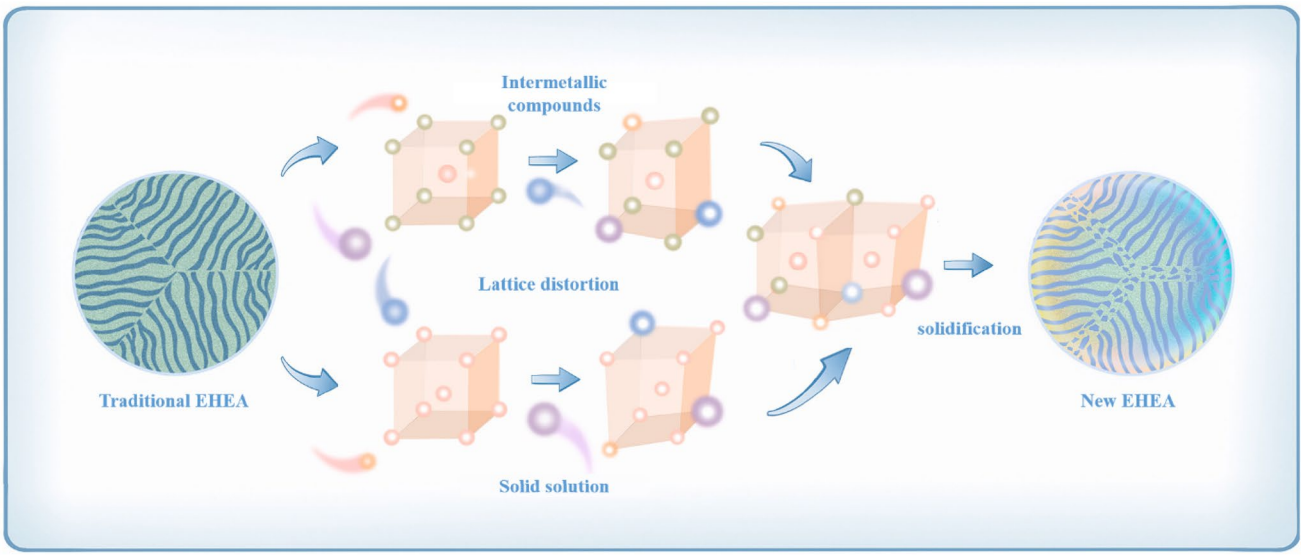

Fig. 6 Schematic diagram of new EHEA designed by partial similarity substitution method [72]

$AlCoCrFeNi_{2.1}$. A Co-free $AlCrFe_{1.5}Ni_{2.6}$ EHEA composed of $L1_2$ and *B2* phases was designed according to this VEC criterion. According to the idea of a simple mixing method, Fang et al. [71] categorized the EHEA elements into two groups: A and B. Group A contains elements with similar atomic radii and chemical properties, resulting in a mixing enthalpy that is nearly zero, these elements have a tendency to form stable solid solutions [72]. On the contrary, the mixing enthalpy of group B elements is relatively negative, and the difference in atomic radius is relatively large, so it is easy to form a stable phase. Then, by finding the composition of the eutectic point in the binary phase diagram, a new type of cost-effective FeNi-based EHEAs was successfully proposed, and $[FeNi]_{65}Cr_{15}Mn_{10}Nb_{10}$ has a complete eutectic composition experimentally. Similarly, Li et al. [72] designed a new EHEA by replacing similar elements. Mainly based on a known EHEA, it causes lattice distortion through partial element substitution to form a new EHEA. The main idea is shown in Fig. 6.

6 Conclusion and Outlook

In this paper, we review the factors influencing the phase formation thermodynamics of EHEAs and computationally verify their current guiding role. The alloy design strategies and research progress that have been reported in recent years are reviewed. In the process of designing the composition of EHEAs, in addition to considering the internal factors of thermodynamics and the solidification process, external factors such as its cost-effectiveness should also be considered. Therefore, in addition to maintaining its excellent performance in mechanical properties, it is also necessary to consider its cost control. The lack of a complete database and the amount of experimental data bring challenges to the composition design of EHEAs.

Declarations

Conflict of interest All authors have no conflict of interest to report.

References

1. Yeh J W, Chen S K, Lin S J, Gan J Y, Chin T S, Shun T T, Tsau C H, and Chang S Y, *Adv Eng Mater* **6** (2004) 299. https://doi.org/10.1002/adem.200300567
2. Yeh J W, *Ann Chim Sci Matér* **31** (2006) 633. https://doi.org/10.3166/acsm.31.633-648
3. Ye Y F, Wang Q, Lu J, Liu C T, and Yang Y, *Mater Today* **19** (2016) 349. https://doi.org/10.1016/j.mattod.2015.11.026
4. Murty B S, Yeh J W, Ranganathan S, and Bhattacharjee P, *High-Entropy Alloys*. Elsevier, Amsterdam (2019).
5. Lu Y, Dong Y, Jiang H, Wang Z, Cao Z, Guo S, Wang T, Li T, and Liaw P K, *Scr Mater* **187** (2020) 202. https://doi.org/10.1016/j.scriptamat.2020.06.022
6. Zhang Z, Ma P, Fang Y, Yang Z, Zhang N, Prashanth K G, and Jia Y, *J Alloys Compd* **947** (2023) 169417. https://doi.org/10.1016/j.jallcom.2023.169417
7. Ma P, Fang Y, Wei S, Zhang Z, Yang H, Wan S, Prashanth K G, and Jia Y, *J Mater Res Technol* **25** (2023) 7090. https://doi.org/10.1016/j.jmrt.2023.07.124
8. Lu Y, Dong Y, Guo S, Jiang L, Kang H, Wang T, Wen B, Wang Z, Jie J, Cao Z, Ruan H, and Li T, *Sci Rep* **4** (2014) 6200. https://doi.org/10.1038/srep06200

9. Maity T, Prashanth K G, Balcı Ö, Kim J T, Schöberl T, Wang Z, and Eckert J, *Int J Plast* **109** (2018) 121. https://doi.org/10.1016/j.ijplas.2018.05.012
10. Maity T, Prashanth K G, Balçi Ö, Wang Z, Jia Y D, and Eckert J, *Compos Part B Eng* **150** (2018) 7. https://doi.org/10.1016/j.compositesb.2018.05.033
11. Glicksman M E, *Principles of Solidification: an Introduction to Modern Casting and Crystal Growth Concepts*, Springer Science & Business Media, New York (2010).
12. Chanda B, and Das J, *J Alloys Compd* **798** (2019) 167. https://doi.org/10.1016/j.jallcom.2019.05.241
13. Yang X, and Zhang Y, *Mater Chem Phys* **132** (2012) 233. https://doi.org/10.1016/j.matchemphys.2011.11.021
14. Zhang Y, Zhou Y J, Lin J P, Chen G L, and Liaw P K, *Adv Eng Mater* **10** (2008) 534.
15. Jin X, Zhou Y, Zhang L, Du X, and Li B, *Mater Des* **143** (2018) 49. https://doi.org/10.1016/j.matdes.2018.01.057
16. Jiang H, Han K, Gao X, Lu Y, Cao Z, Gao M C, Hawk J A, and Li T, *Mater Des* **142** (2018) 101. https://doi.org/10.1016/j.matdes.2018.01.025
17. Jiao W, Miao J, Lu Y, Chen X, Ren Z, Yin G, and Li T, *J Alloys Compd* **941** (2023) 168975. https://doi.org/10.1016/j.jallcom.2023.168975
18. Lu Y, Jiang H, Guo S, Wang T, Cao Z, and Li T, *Intermetallics* **91** (2017) 124. https://doi.org/10.1016/j.intermet.2017.09.001
19. Tan Y, Li J, Wang J, and Kou H, *Intermetallics* **85** (2017) 74. https://doi.org/10.1016/j.intermet.2017.02.004
20. He F, Wang Z, Cheng P, Wang Q, Li J, Dang Y, Wang J, and Liu C T, *J Alloys Compd* **656** (2016) 284. https://doi.org/10.1016/j.jallcom.2015.09.153
21. Rahul M R, and Phanikumar G, *Metall Mater Trans A* **50** (2019) 2594. https://doi.org/10.1007/s11661-019-05210-3
22. Wu M, Wang S, Huang H, Shu D, and Sun B, *Mater Lett* **262** (2020) 127175. https://doi.org/10.1016/j.matlet.2019.127175
23. Mukarram M, Mujahid M, and Yaqoob K, *J Mater Res Technol* **10** (2021) 1243. https://doi.org/10.1016/j.jmrt.2020.12.042
24. Vikram R J, Gupta K, and Suwas S, *Scr Mater* **202** (2021) 113993. https://doi.org/10.1016/j.scriptamat.2021.113993
25. Gasan H, and Ozcan A, *Met Mater Int* **26** (2020) 1152. https://doi.org/10.1007/s12540-019-00515-9
26. Ai C, He F, Guo M, Zhou J, Wang Z, Yuan Z, Guo Y, Liu Y, and Liu L, *J Alloys Compd* **735** (2018) 2653. https://doi.org/10.1016/j.jallcom.2017.12.015
27. Jain R, Dewangan S K, Kumar V, and Samal S, *Mater Sci Eng A* **797** (2020) 140059. https://doi.org/10.1016/j.msea.2020.140059
28. Wen X, Cui X, Jin G, Liu Y, Zhang Y, and Fang Y, *Surf Coat Technol* **405** (2021) 126728. https://doi.org/10.1016/j.surfcoat.2020.126728
29. Yurchenko N, Panina E, Zherebtsov S, and Stepanov N, *Materialia* **16** (2021) 101057. https://doi.org/10.1016/j.mtla.2021.101057
30. Ali Shafiei A, *Met Mater Int* **27** (2021) 127. https://doi.org/10.1007/s12540-020-00655-3
31. Wang L, Yao C, Shen J, Zhang Y, Liu G, Wu X, and Zhang G, *Mater Sci Eng A* **830** (2022) 142325. https://doi.org/10.1016/j.msea.2021.142325
32. Jin X, Bi J, Zhang L, Zhou Y, Du X, Liang Y, and Li B, *J Alloys Compd* **770** (2019) 655. https://doi.org/10.1016/j.jallcom.2018.08.176
33. Dong Y, Yao Z, Huang X, Du F, Li C, Chen A, Wu F, Cheng Y, and Zhang Z, *J Alloys Compd* **823** (2020) 153886. https://doi.org/10.1016/j.jallcom.2020.153886
34. Yin Y, Kent D, Tan Q, Bermingham M, and Zhang M-X, *J Mater Sci Technol* **51** (2020) 173. https://doi.org/10.1016/j.jmst.2020.01.066
35. Jiao W, Jiang H, Qiao D, He J, Zhao H, Lu Y, and Li T, *Mater Chem Phys* **260** (2021) 124175. https://doi.org/10.1016/j.matchemphys.2020.124175
36. Ye X, Xiong J, Wu X, Liu C, Xu D, Zhang W, Fang D, and Li B, *Scr Mater* **199** (2021) 113886. https://doi.org/10.1016/j.scriptamat.2021.113886
37. Shah N, Rahul M R, and Phanikumar G, *Metall Mater Trans A* **52** (2021) 1574. https://doi.org/10.1007/s11661-021-06218-4
38. Liu F, Xiao X, Huang L, Tan L, and Liu Y, *Mater Today Commun* **30** (2022) 103172. https://doi.org/10.1016/j.mtcomm.2022.103172
39. Wu H, Xie J, Yang H, Shu D, Hou G, Li J, Zhou Y, and Sun X, *J Mater Res Technol* **19** (2022) 1759. https://doi.org/10.1016/j.jmrt.2022.05.165
40. Liu Q, Liu X, Fan X, Li R, Tong X, Yu P, and Li G, *J Alloys Compd* **904** (2022) 163775. https://doi.org/10.1016/j.jallcom.2022.163775
41. Takeuchi A, and Inoue A, *Mater Trans* **46** (2005) 2817. https://doi.org/10.2320/matertrans.46.2817
42. He F, Wang Z, Ai C, Li J, Wang J, and Kai J J, *Mater Chem Phys* **221** (2019) 138. https://doi.org/10.1016/j.matchemphys.2018.09.044
43. Kim M J, Kang G C, Hong S H, Park H J, Mun S C, Song G, and Kim K B, *J Mater Sci Technol* **57** (2020) 131. https://doi.org/10.1016/j.jmst.2020.03.045
44. Kittel C, *Introduction to Solid State Physics*, 8th edn. Wiley, Hoboken (2005).
45. Guo S, Ng C, Lu J, and Liu C T, *J Appl Phys* **109** (2011) 103505. https://doi.org/10.1063/1.3587228
46. Chen X, Sui Y, Qi J, He Y, Wei F, Meng Q, and Sun Z, *J Mater Res* **32** (2017) 2109. https://doi.org/10.1557/jmr.2017.10
47. Jin X, Zhou Y, Zhang L, Du X, and Li B, *Mater Lett* **216** (2018) 144. https://doi.org/10.1016/j.matlet.2018.01.017
48. Wang M, Lu Y, Wang T, Zhang C, Cao Z, Li T, and Liaw P K, *Scr Mater* **204** (2021) 114132. https://doi.org/10.1016/j.scriptamat.2021.114132
49. Jiang H, Qiao D, Jiao W, Han K, Yiping L, and Liaw P K, *J Mater Sci Technol* **61** (2021) 119. https://doi.org/10.1016/j.jmst.2020.05.053
50. Wang M, Lu Y, Lan J, Wang T, Zhang C, Cao Z, Li T, and Liaw P K, *Acta Mater* **248** (2023) 118806. https://doi.org/10.1016/j.actamat.2023.118806
51. Gwalani B, Wang T, Jagetia A, Gangireddy S, Muskeri S, Mukherjee S, Lloyd J T, Banerjee R, and Mishra R S, *Entropy* **22** (2020) 431. https://doi.org/10.3390/e22040431
52. Dong Y, Jiang L, Jiang H, Lu Y, Wang T, and Li T, *Mater Des* **82** (2015) 91. https://doi.org/10.1016/j.matdes.2015.05.046
53. Yu Y, He F, Qiao Z, Wang Z, Liu W, and Yang J, *J Alloys Compd* **775** (2019) 1376. https://doi.org/10.1016/j.jallcom.2018.10.138
54. Jiang H, Qiao D, Lu Y, Ren Z, Cao Z, Wang T, and Li T, *Scr Mater* **165** (2019) 145. https://doi.org/10.1016/j.scriptamat.2019.02.035
55. Tillmann W, Wojarski L, Stangier L, Manka M, and Timmer C, *Weld World* **64** (2020) 1597. https://doi.org/10.1007/s40194-020-00944-w
56. Huo W, Zhou H, Fang F, Xie Z, and Jiang J, *Mater Des* **134** (2017) 226. https://doi.org/10.1016/j.matdes.2017.08.030
57. Huo W, Zhou H, Fang F, Zhou X, Xie Z, and Jiang J, *J Alloys Compd* **735** (2018) 897. https://doi.org/10.1016/j.jallcom.2017.11.075
58. Ai C, Wang G, Liu L, Guo M, He F, Zhou J, Chen Y, Wang Z, and Gan B, *Intermetallics* **120** (2020) 106769. https://doi.org/10.1016/j.intermet.2020.106769
59. Guo Y, Liu L, Zhang Y, Qi J, Wang B, Zhao Z, Shang J, and Xiang J, *J Mater Res* **33** (2018) 3258. https://doi.org/10.1557/jmr.2018.177

60. Jiang H, Zhang H, Huang T, Lu Y, Wang T, and Li T, *Mater Des* **109** (2016) 539. https://doi.org/10.1016/j.matdes.2016.07.113
61. Samal S, Rahul M R, Kottada R S, and Phanikumar G, *Mater Sci Eng A* **664** (2016) 227. https://doi.org/10.1016/j.msea.2016.04.006
62. Jain R, Umre P, Sabat R K, Kumar V, and Samal S, *J Mater Eng Perform* **31** (2022) 8124. https://doi.org/10.1007/s11665-022-06829-x
63. Jiang L, Lu Y, Wu W, Cao Z, and Li T, *J Mater Sci Technol* **32** (2016) 245. https://doi.org/10.1016/j.jmst.2015.08.006
64. Wu Q, Wang Z, Zheng T, Chen D, Yang Z, Li J, Kai J J, and Wang J, *Mater Lett* **253** (2019) 268. https://doi.org/10.1016/j.matlet.2019.06.067
65. Han L, Xu X, Li Z, Liu Z, Liu C T, and Liu Y, *Mater Res Lett* **8** (2020) 373. https://doi.org/10.1080/21663831.2020.1772395
66. Zhang Y, Lu Z P, Ma S G, Liaw P K, Tang Z, Cheng Y Q, and Gao M C, *MRS Commun* **4** (2014) 57. https://doi.org/10.1557/mrc.2014.11
67. Ding Z, He Q, and Yang Y, *Sci China Technol Sci* **61** (2018) 159. https://doi.org/10.1007/s11431-017-9051-6
68. Xie T, Xiong Z, Xu Z, and Cheng X, *Mater Sci Eng A* **786** (2020) 139420. https://doi.org/10.1016/j.msea.2020.139420
69. Xie T, *Mater Sci* **802** (2021) 140634.
70. Mukarram M, Munir M A, Mujahid M, and Yaqoob K, *Metals* **11** (2021) 1484.
71. Fang D, Wu X, Xu W, Yu L, Liu M, Zhang A, Li B, and Ye X, *Mater Sci Eng A* **870** (2023) 144919. https://doi.org/10.1016/j.msea.2023.144919
72. Li J H, and Tsai M H, *Scr Mater* **188** (2020) 80. https://doi.org/10.1016/j.scriptamat.2020.06.064